UC Merced

UC Merced Previously Published Works

Title

Tracking differential activation of primary and supplementary motor cortex across timing tasks: An fNIRS validation study

Permalink

https://escholarship.org/uc/item/9rh9z7jd

Authors

Rahimpour, Ali
Pollonini, Luca
Comstock, Daniel
et al.

Publication Date

2020-07-01

DOI

10.1016/j.jneumeth.2020.108790

Peer reviewed

eScholarship.org Powered by the California Digital Library
University of California

Journal of Neuroscience Methods 341 (2020) 108790

Contents lists available at ScienceDirect

Journal of Neuroscience Methods

journal homepage: www.elsevier.com/locate/jneumeth

Tracking differential activation of primary and supplementary motor cortex across timing tasks: An fNIRS validation study

Ali Rahimpour[a], Luca Pollonini[b], Daniel Comstock[c], Ramesh Balasubramaniam[c], Heather Bortfeld[a,c,*]

[a] Psychological Sciences, University of California, Merced, CA, United States
[b] Departments of Engineering Technology and Electrical and Computer Engineering, University of Houston, TX, United States
[c] Cognitive & Information Sciences, University of California, Merced, CA, United States

ARTICLE INFO

Keywords:
fNIRS
Simple motor timing task
Temporal motor task
Finger tapping task
Continuation paradigm
HRF
AR-IRLS
Canonical statistical analysis

ABSTRACT

Functional near-infrared spectroscopy (fNIRS) provides an alternative to functional magnetic resonance imaging (fMRI) for assessing changes in cortical hemodynamics. To establish the utility of fNIRS for measuring differential recruitment of the motor network during the production of timing-based actions, we measured cortical hemodynamic responses in 10 healthy adults while they performed two versions of a finger-tapping task. The task, used in an earlier fMRI study (Jantzen et al., 2004), was designed to track the neural basis of different timing behaviors. Participants paced their tapping to a metronomic tone, then continued tapping at the established pace without the tone. Initial tapping was either synchronous or syncopated relative to the tone. This produced a 2 × 2 design: synchronous or syncopated tapping and pacing the tapping with or continuing without a tone. Accuracy of the timing of tapping was tracked while cortical hemodynamics were monitored using fNIRS. Hemodynamic responses were computed by canonical statistical analysis across trials in each of the four conditions. Task-induced brain activation resulted in significant increases in oxygenated hemoglobin concentration (oxy-Hb) in a broad region in and around the motor cortex. Overall, syncopated tapping was harder behaviorally and produced more cortical activation than synchronous tapping. Thus, we observed significant changes in oxy-Hb in direct relation to the complexity of the task.

1. Introduction

The human motor system dynamically controls different movement sequences across a range of complexities, including the number of limbs used, number of trajectories followed, sequence length, and timing relative to external stimuli (Wolpert and Ghahramani, 2000). In particular, the ability to accurately and precisely perform time-dependent behavior is critical for a variety of skills, such as playing sports or playing a musical instrument. A large body of research has advanced our understanding of how temporal mechanisms control action, with recent work focusing on the representation of timing in the central nervous system. Finger tapping is a task that is reliable and thus is commonly used for measuring motor performance, and evaluating muscle control and motor ability in the upper extremities (Repp, 2005). It has also been used to probe the neural representation and maintenance of timing behavior and to measure relative changes in cortical hemodynamics while participants perform tapping tasks with systematically varied levels of difficulty (Spencer et al., 1998). Studies of finger tapping thus allow investigation of the mental timing system not associated with complicated motor implementation or feedback mechanisms (Ivry and Keele, 1989; Sergent, 1993; Wing and Kristofferson, 1973). In the current study, we use a modified finger tapping task (Jantzen et al., 2004), together with functional near-infrared spectroscopy (fNIRS), to build on previous work delineating the timing mechanisms underlying complex motor behavior (Balasubramaniam et al., 2004; Cluff et al., 2010; Ross and Balasubramaniam, 2014; Studenka et al., 2012).

One such motor behavior is sensory-motor synchronization, or the matching of a body rhythmic movement to on external rhythmic stimulus. Although tasks in motor research most often involve finger tapping, sensory-motor synchronization can range from finger tapping in time with a metronome to musical ensemble performance (Repp and Su, 2013). Depending on the level of difficulty of the specific task, finger tapping generally recruits primary sensory and motor cortices (S1 and M1), supplementary motor area (SMA), premotor cortex (PMC), inferior parietal cortex (IPL), basal ganglia, and cerebellum (Witt et al.,

* Corresponding author at: Psychological Sciences & Cognitive and Information Sciences, University of California, Merced, CA, United States.
E-mail address: hbortfeld@ucmerced.edu (H. Bortfeld).

https://doi.org/10.1016/j.jneumeth.2020.108790
Received 28 January 2020; Received in revised form 25 April 2020; Accepted 17 May 2020
Available online 19 May 2020
0165-0270/ © 2020 Elsevier B.V. All rights reserved.

2008), with different task-specific parameters modulating the specific neural mechanisms engaged. For example, although SMA is involved primarily in motor planning, its activity also reflects an active supervisory role of M1 during motor processing (Kasess et al., 2008). The more complex the task, the more SMA is engaged. Thus, moving from tapping a finger synchronously with a rhythmic stimulus to syncopating tapping relative to the stimulus results in greater engagement of M1 and broader engagement of regions beyond the primary motor networks, including SMA (Byblow and Stinear, 2006; J. L. Chen et al., 2008; Jantzen et al., 2004; Mayville et al., 2002). Similarities and differences in the neural circuits engaged during different kinds of tapping can be further investigated by adding a pacing-continuation component to the task (Wing and Kristofferson, 1973): synchronized finger tapping engages the motor-cerebellar network, continuation of synchronized tapping without an accompanying sound engages a broader range of cortical regions due to its load on working memory, among other things. Motor areas such as M1, S1, SMA, and anterior cerebellum are commonly activated during both pacing and continuation tapping (Witt et al., 2008). Thus, more complex tasks result in greater activation in cortical areas beyond M1, as well as in stronger coupling to the area processing the external stimulus (e.g., primary auditory cortex (A1), in the case of a rhythmic tone).

In their study, Jantzen and colleagues (Jantzen et al., 2004) used functional magnetic resonance imaging (fMRI) to track changes in cortical and subcortical hemodynamics as participants performed finger tapping with systematically varied levels of timing difficulty. Their primary goal was to establish whether the neural activity underlying timing behavior depends on the initial pacing context or is independent of that context. Thus, they compared the neural networks engaged when participants performed synchronized pacing followed by synchronized continuation to those engaged during syncopated pacing followed by syncopated continuation. Crucially, if the areas supporting continuation are independent of the method for establishing the pacing, then the researchers should have observed no difference between the synchronized or syncopated continuation phases of their study. Rather, and consistent with their hypothesis, they found that such contextual framing of participants' tapping behavior did influence the neural regions that were engaged: syncopated continuation involved more and broader activation of motor networks than synchronized continuation. Despite the tapping behavior looking essentially identical during both continuation phases, fMRI revealed that the neural networks engaged in the syncopated continuation condition were broader than those in the synchronized continuation condition.

While fMRI is the gold standard for assessing whole-brain hemodynamics, fNIRS provides a low-cost alternative for researchers interested in measuring cortex-specific hemodynamics. Although limited to the cortex, fNIRS has certain advantages over other neuroimaging methods. It has a higher temporal resolution than fMRI and positron emission tomography (PET), and better spatial resolution than electroencephalogram (EEG). Moreover, other recording techniques are highly affected by movement while fNIRS is less so. As such, fNIRS has been used to delineate the neural mechanisms underlying a range of perceptual and cognitive processes (e.g., Borjkhani and Setarehdan, 2020; Bortfeld et al., 2009, 2007; Chen et al., 2011; Mirbagheri et al., 2019; Ebrahimzadeh et al., 2019; Jahani et al., 2015; Mirbagheri et al., 2020; Pollonini et al., 2014; Rahimpour et al., 2017, 2018). Here we extend the findings of Jantzen and colleagues (Jantzen et al., 2004) to fNIRS, with the goal of establishing whether fNIRS is spatially and temporally sensitive enough to differentiate activation in the different cortex-specific regions of interest identified by Jantzen et al. to be differentially engaged by synchronized and syncopated finger tapping.

Thus, the current study represents an attempt to use fNIRS to reproduce findings previously obtained using fMRI (Jantzen et al., 2004). Similar fMRI replication attempts using fNIRS have focused on working memory networks (Wijeakumar et al., 2017), neurocognitive processes associated with neurological and psychiatric disorders (Irani et al., 2007) and naturalistic full-body activities and behaviors (Noah et al., 2015). Here we asked participants to produce timing behavior similar to that used by Jantzen et al. (Jantzen et al., 2004). As with the original study, our task took place in two phases. First, participants paced their tapping to a metronomic tone ('pacing'), then continued tapping at the established pace without the tone ('continuation'). They were instructed to tap either in a synchronous or syncopated manner relative to the tone. This produced a 2 × 2 design: synchronous/syncopated tapping to the tone; pacing with/continuing without the tone. The temporal accuracy of participants' tapping was tracked while their cortical hemodynamics were monitored using fNIRS. Hemodynamic responses were computed by canonical statistical analysis across trials in each of the four conditions. We predicted that the synchronized finger-tapping task would recruit primary auditory (A1) and motor cortex (M1), SMA, PMC, and inferior parietal and temporal cortex (Witt et al., 2008), while syncopation (a more complex timing behavior) would engage a broader network of cortical regions and result in greater levels of cortical activation overall (Jantzen et al., 2004). We also predicted that continuation would result in greater activation of SMA relative to pacing (Lewis et al., 2004), while activation of the superior temporal gyrus (STG) would be present during pacing and not during continuation.

2. Materials and methods

2.1. Participants

Twelve healthy non-musically trained participants were recruited. Data from two participants were not analyzed due to overtly poor signal quality. Thus, ten healthy right-handed adult volunteers (mean age 22.5, range 19–25) at the University of California, Merced successfully participated in the study. No participants reported any neurological or skeletomuscular disorder or injury that would prevent them from performing a timing-based tapping task. The protocol was approved by the Institutional Review Board for research ethics and protection of human subjects at the University of California, Merced. All participants gave informed consent after the experimental procedures were explained to them.

2.2. Task

Our experimental protocol closely followed that used by Jantzen and colleagues (2004). While seated in a comfortable chair, participants performed tapping movements with the index finger of their right (dominant) hand in response to a 20 ms long, 1 kHz metronomic tone that occurred every 1000 ms (1 Hz). The task (see Fig. 1) involved two patterns of tone-guided tapping: taps synchronized with the tone and taps syncopated relative to the tone (that is, in between the tones, or "off beat"). To adjust for the change in participant positioning (i.e., from supine to seated) due to the transition from fMRI to fNIRS, which pilot work revealed made the task somewhat more difficult, we slowed the tapping pace slightly from Jantzen et al.'s original 1.25 Hz to 1 Hz. Participants completed a total of 20 trials, 10 trials per tapping pattern. Trials were blocked by tapping pattern and pattern order was counterbalanced across participants. Within each trial, regardless of tapping pattern, tapping took place in two phases: pacing with the tone (15 cycles) and continuing without the tone (12 cycles). Distinct from Jantzen et al.'s design, an additional three cycles were added to the pacing phase to give participants additional time to entrain to the tapping pattern prior to the no-tone continuation phase. Moreover, we slowed the rate of tones (1 Hz vs. 1.25 Hz) to simplify the task. A 1 s long tone indicated the end of a trial and the start of a 20 s no-tapping rest period.

To register the timing of each tap relative to the tone, participants tapped with their right index finger on a metal plate. The metal plate was a custom-built electronic input device produced from a MakeyMakey™ kit (Comstock and Balasubramaniam, 2018) with a lead

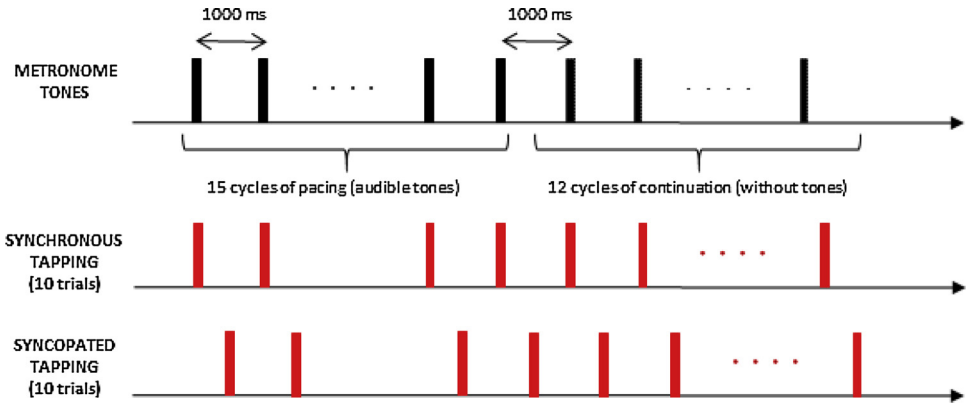

Fig. 1. Schematic of the experimental paradigm to perform repetitive right finger tapping in the presence of an auditory metronome that produced a one kHz tone for 20 ms every 1 Hz. The task consisted of 20 tapping trials. Each trial began with a pacing phase (15 cycles of tapping with the tone, with the first three as warm ups and not included in analyses) followed by a continuation phase (12 tapping cycles continued in the same manner established during pacing but without the tone). Two different tapping patterns were performed: synchronized with or syncopated to the tone. Ten trials of each tapping pattern were performed, with trials blocked by tapping pattern. During each trial, participants fixated a crosshair (+).

to a computer. The MakeyMakey device connected to the data acquisition computer via USB, with polling rate determined by the USB controller (i.e., 1000 samples per second). When the subject touched the metal plate, it completed a circuit in the input device, sending a signal to the computer to register a tap (Collective and Shaw, 2012).

The onset of each behavioral response was defined as the point at which a participant's finger tapped the plate, with the time of each response corrected by 25 ms to account for the device's temporal delay. This 25 ms delay is due in part to the time it takes the internal circuitry of the MakeyMakey™ to process the input, a built-in delay for input registration that reduces accidental double inputs (similar to a computer keyboard). There is also a short delay for the computer to process the input before it is registered. The 25 ms delay was measured via a method suggested by MakeyMakey™ engineers: we used a high speed camera (240 fps) to simultaneously record the timing of the tap and the timing of the computer registration of that tap via a tone output from the computer. This revealed a delay of approximately 25 ms (+/−2 ms from the camera frame rate).

From this, two relative measures of performance were calculated: inter-response interval (IRI) was defined as the time between consecutive tapping, and relative timing (phase) was defined as the time difference between each response and the preceding stimulus onset (Jantzen et al., 2004). Thus, we were able to analyze the accuracy of tapping across the four conditions by converting the IRIs to the phase categorical predictor. Phase 0° corresponds to precise tapping on the tones, and phase 180° represents tapping precisely between two tones (i.e., precise syncopation).

2.3. fNIRS data acquisition

fNIRS provides an alternative to fMRI for assessing hemodynamics specific to the cortex. The NIRS method is based on changes in near-infrared light absorption reflecting corresponding concentration changes in oxygenated (oxy-Hb) and deoxygenated (deoxy-Hb) hemoglobin in the cortex (Abdelnour and Huppert, 2009; Jahani et al., 2015; Pollonini et al., 2014; Rahimpour, Dadashi, Soltanian-Zadeh, et al., 2017; Rahimpour, Noubari, et al., 2018). We used a two-wavelength fNIRS system (NIRScout, NIRx, Glen Head, NY) with 16 light-incident emitters; 20 light-detecting fibers, and a sampling rate of 6.25 Hz. The light sources were continuous LEDs with wavelengths of 760 and 850 nm coupled in each emitter. The depth of fNIRS measurements (with probes placed externally on the scalp) depends on the distance between the transmitters and the receivers. It is reported that the NIRS signal reflects the absorption at a depth of 1.2–2 cm from the scalp when the inter-probe distance is 2.7 cm (Kobayashi et al., 2006; Raichle, 1994). As the human cerebral cortex usually lies about 1.0–2.0 cm deep from the scalp, the suitable inter-probe distance should be about 2.5–3.0 cm to measure the activities of the cerebral surface in an adult. The optodes were positioned according to the 10:10 EEG system used for standard electrode positions, which were set with inter-probe distance at 3.0 cm.

2.4. Statistical analyses

For data analysis, we used the NIRS Brain AnalyzIR toolbox (https://github.com/huppertt/nirs-toolbox) (Santosa et al., 2018), an open-source MATLAB-based (Mathworks, Natick, MA, USA) analysis package designed for fNIRS data management, pre-processing, and statistical analysis. fNIRS data and its source of noise have unique properties that require adjustment of statistical methods in order to control type-I error (false positive) accurately. The underlying logic for the development of the AnalyzIR toolbox was to create a statistical analysis package to address the properties of fNIRS data specifically.

Because it is helpful to represent the activated brain areas on a visualization model, we mapped our channels onto a brain schematic. Fig. 2 shows our fNIRS channel placement and measurement sensitivity. Channel positions are mapped relative to typical 10:10 scalp landmarks. The sensitivity map is derived from photon migration simulations of our probe on a 3D model of a human head. Sensitivity was computed and displayed with AtlasViewer (Aasted et al., 2015).

In order to calculate hemodynamic responses based on the fNIRS data, the raw data first was transformed from optical density units to oxy- and deoxygenated hemoglobin concentrations using the modified Beer–Lambert Law (Bortfeld et al., 2009, 2007; Chen et al., 2011; Jahani et al., 2015; Pollonini et al., 2014; Rahimpour, Dadashi, Soltanian-Zadeh, et al., 2017; Rahimpour, Noubari, et al., 2018). The mean of the fNIRS signal acquired at each channel during each of the four test conditions was estimated relative to the mean of the fNIRS signal during a pre-baseline period by using a regression model and computed using an autoregressive iterative reweighted least square (AR-IRLS) algorithm (Huppert, 2016; Karim et al., 2014). The AR-IRLS method automatically accounts for the expected presence of extracerebral components in the optical signals due to cardiac pulsation and respiration, and it automatically excludes movement artifacts as statistical outliers. Hence, a bandpass signal filtering step was not explicitly required to remove these components. This algorithm iteratively reweighted all terms to minimize the effect of outliers using both prewhitening and robust regression, thus making the algorithm robust to physiological and motion artifacts (Hoppes et al., 2018; Lin et al., 2017).

We used a canonical model to estimate the regression coefficients of the general linear model and, finally, to generate the hemodynamic response functions (HRFs). In our analyses, we only consider the significantly active channels with p-value lower than 5% (i.e., statistically non-zero β). The statistically significant activations were computed on a per-participant and per-channel basis, and these results were used for a second, group-level analysis. Group-level analyses were performed via a linear mixed-effects model that included β per channel (dependent

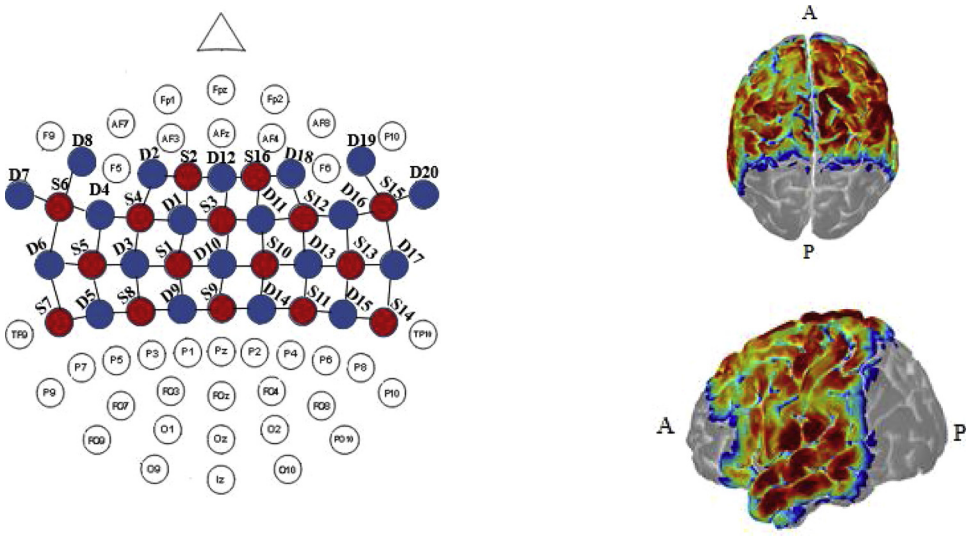

Fig. 2. fNIRS channel placement and sensitivity maps. Depiction of geometrical layout of sources (S, red) and detectors (D, blue) with respect to the international 10-10 EEG system (left) and the corresponding sensitivity maps (right) derived from photon migration simulations of probe in a 3D head model overlaid onto the AtlasViewer model (see Materials and Methods for details). A and P indicate anterior and posterior, respectively. (For interpretation of the references to color in this figure legend, the reader is referred to the web version of this article.)

variable) and conditions (independent variable) to model group-level correlations (Abdelnour and Huppert, 2009).

The fNIRS measurement positions were registered to an anatomical AtlasViewer using a custom registration algorithm interfacing with the international 10:10 coordinate system. For each channel, estimates of the regression coefficients, β, for oxy-Hb and deoxy-Hb, were computed for each subject and trial. Here we focus our analyses on oxy-Hb since it provides the more consistent measures of the two chromophores and higher signal-to-noise ratios than deoxy-Hb, reduced inter-subject variability, and reduced vulnerability to contamination (Wilson et al., 2014).

Our goal statistically was to determine the weights β for all 55 channels, thus describing the brain activation strength at each. To compare activation across the four different conditions, we performed t-tests between the computed HRFs using the false discovery rate method to adjust the type-I error rate (α) (Santosa et al., 2017). We report behavioral results, followed by comparison of fNIRS-based average activation maps and their corresponding coordinates in the 10 − 10 EEG system landmarks (Fig. 2) for each condition in the Jantzen et al. study. We then compare our hemodynamic response functions for the three main areas of interest to those reported by Jantzen and colleagues, ending with a comparison of our contrast maps (synchronization vs. syncopation; pacing vs. continuation) to those reported in Jantzen et al. (2004).

3. Results

3.1. Behavioral results

Fig. 3 shows the IRI and standard deviation for the four conditions, first from Jantzen et al. (2004) (Figs. 3A and B, respectively) and for our study (Figs. 3C and D, respectively). For synchronized and syncopated pacing, the average relative phases were 15.1± 29.9° (mean ± SD) and 169.5± 57.1°, respectively. Besides, the estimation of the average continuation phase relative to that with the metronome was 20.4 ± 17.7° for synchronization and 194.24 ± 46.9° for syncopation.

Our data show synchronization behavior (filled bars) performed with a mean IRI of 1005 ± 22.1 ms and 991 ± 26.8 ms for the pacing and continuation phases, respectively. The average response rate was slightly slower than the metronome, with mean IRIs of 1054 ± 24.1 ms for pacing and 1140 ± 29.6 ms for continuation. We performed a two-way ANOVA on the IRIs by using pattern (synchronization, syncopation) and phase (pacing, continuation) as our two factors, finding main effects for both tapping pattern, $F(1,18) = 3.23$, $p < 0.05$, and phase, $F(1,18) = 3.81$, $p < 0.04$. Overall performance was better (more accurate) for the synchronization than syncopation conditions, with mean performance in the syncopated continuation condition the poorest of the four (138.9°, Fig. 3C). An interaction also revealed a significant difference between IRI means for the synchronized pacing and syncopated continuation conditions, $F(118) = 3.75$, $p < 0.05$.

Accuracy across conditions reveals similar stability, as reflected in the mean SD (Fig. 3B). SDs across conditions were 69 ± 22.36 (synchronized pacing), 72.39 ± 18.6 (syncopated pacing), 79.73 ± 38.3 synchronized continuation, and 88.9 ± 42.3 (syncopated continuation).

3.2. Hemodynamic results

In this section we highlight the significant cortical activation effects across the four task conditions.

3.2.1. Synchronized pacing

We observed significant activation of bilateral STG and MTG, $t = 3.24$, $p < 0.005$), with activation in left medial temporal gyrus extending anteriorly into left S1/M1 ($t = 2.9$, $p < 0.015$). Our results also indicate significant activation in bilateral superior and medial frontal gyrus (SFG, MFG) ($t = 3.14$, $p < 0.007$). Finally, there was significant activation in the bilateral posterior parietal cortex (PPC, $t = 3.09$, $p < 0.007$).

3.2.2. Synchronized continuation

Cortical activation patterns during synchronized continuation were similar to those seen during synchronized pacing, with clusters of activation in left S1/M1 ($t = 3.01$, $p < 0.009$) and a small cluster in the left SFG ($t = 2.43$, $p < 0.07$). Where SFG regions were bilaterally activated in the synchronized pacing condition, only the left SFG was activated in the synchronized continuation condition. Moreover, during synchronized continuation, a large cluster of activation appeared in right premotor cortex (PMC) and part of the right inferior parietal lobe (IPL) ($t = 3.3$, $p < 0.001$). Not surprisingly, given the cessation of the tone in this phase, no activation was observed in the temporal regions.

3.2.3. Syncopated pacing

Overall, syncopated pacing engaged a broader network of activation than synchronized pacing, producing additional bilateral activation in both SMA ($t = 2.12$, $p < 0.05$), along with S1/M1 ($t = 2.15$, $p < 0.05$). Activation was also observed in a small cluster of left IPL ($t = 2.1$, $p < 0.05$).

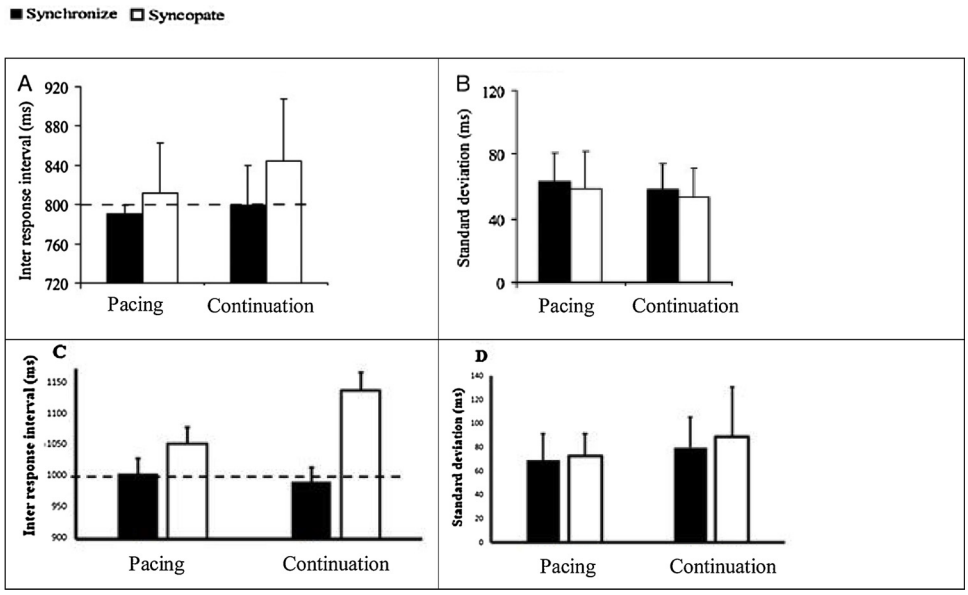

Fig. 3. Figures A/B are adapted from Jantzen et al. (2004); Figure C/D are results from the present study. Figures 3A/C: average time (ms); Figures 3B/D: standard deviations (ms) of inter-response intervals (IRIs) for synchronization (filled) and syncopation (open) conditions. Bars are standard error. Dashed line indicates target response interval.

3.2.4. Syncopated continuation

Broader activation was observed in the syncopated continuation condition relative to the other three conditions in the outer regions of the sensorimotor area, including bilateral SMA ($t = 3.2$, $p < 0.004$) and S1/M1 ($t = 2.24$, $p < 0.05$), left PMC ($t = 2.5$, $p < 0.03$), bilateral superior parietal lobe (SPL) ($t = 2.03$, $p < 0.05$), and right MTG ($t = 1.9$, $p < 0.05$).

3.3. Comparison of hemodynamic response functions across regions of interest

Fig. 4 shows results from both Jantzen et al. (2004) and the current study, illustrating the hemodynamic response functions from the three primary brain regions of interest for this task, including left primary auditory cortex (A1), primary motor cortex (M1), and supplementary motor are (SMA). The fMRI figure shows mean functional time series averaged across voxels and presentation blocks for each region, while the fNIRS data show oxygenated hemodynamic (oxy-Hb) changes averaged across channels for each region. The time course includes pretrial baseline, pacing, and continuation phases for each of the two different tapping patterns. As illustrated, fNIRS-based oxy-Hb responses increase in M1, which shows consistently elevated activation across pacing and continuation phases for both the syncopation and synchronization conditions. There is a small and nonsignificant difference in the fNIRS data between levels of activation for synchronization and syncopation in the continuation phase. In A1, a decrease in oxy-Hb responses is seen at onset of the continuation phase for both the syncopation and synchronization tapping patterns, reflecting the change

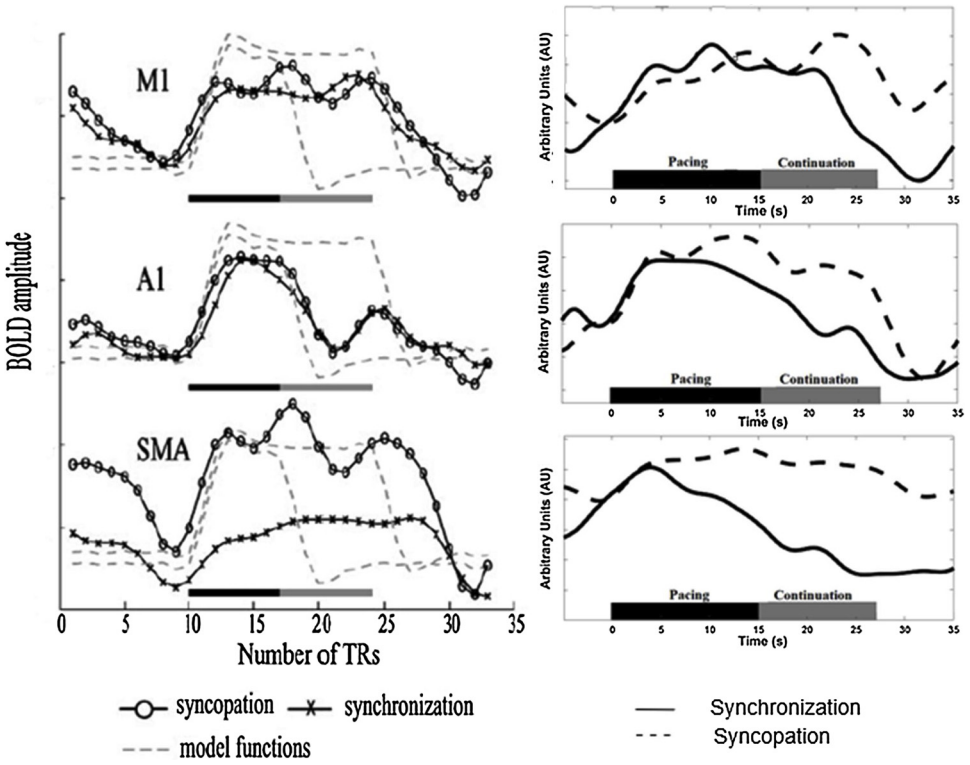

Fig. 4. BOLD responses from Jantzen et al. (2004) (left column), and hemodynamic response functions (right column) for three ROIs: M1, A1/STG, and SMA. Left column: Gray dashed lines show predicted BOLD responses for pacing phase alone (black bar) and pacing and continuation phases together (black + gray bar). Recorded BOLD response for both syncopation (circles) and synchronization (Xs). Vertical axis: BOLD amplitude; horizontal axis: time, shown as scan repetitions (repetition time (TR): 3 s). Right column: fNIRS recorded hemodynamic response (oxy-Hb) for syncopation (dashed line) and synchronization (solid line) across pacing and continuation phases.

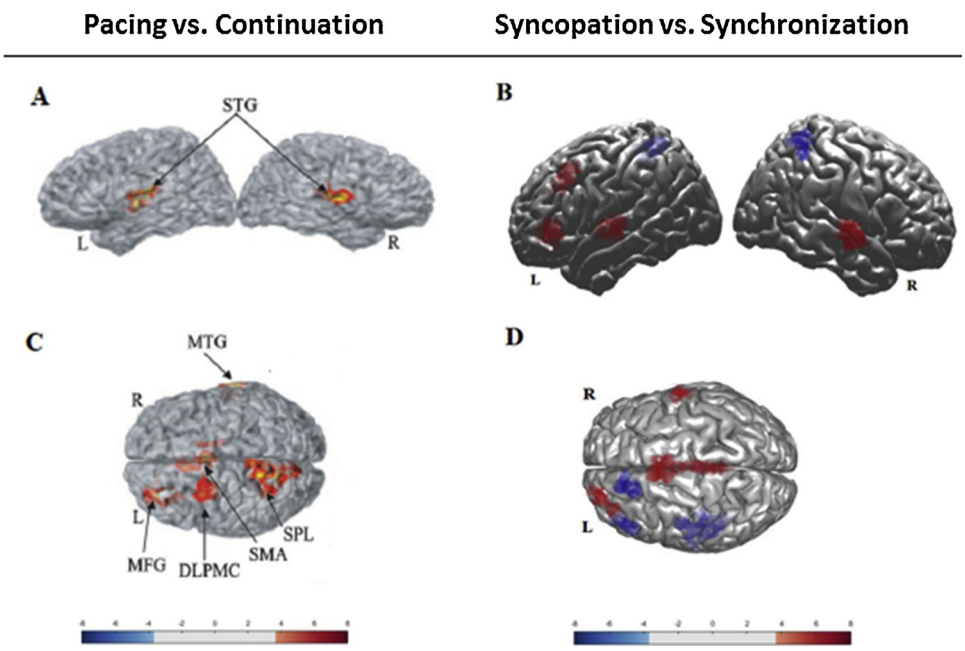

Fig. 5. Fig. 5A/5B: fMRI/fNIRS contrast maps of main effect ($p < 0.05$) for tapping phase (pacing vs. continuation) averaged across tapping pattern from Jantzen et al. (2004) (Fig. 5A), and the current study (Fig. 5B). Fig. 5C/5D: Contrast maps for main effect ($p < 0.05$) of tapping pattern (syncopation vs. synchronization) averaged across tapping phases in Jantzen et al. (2004) (Fig. 5C), and the current study (Fig. 5D). Color bars represent the t-value range (see Tables 1 and 2 for details).

from pacing to the auditory tone to continuing without it. In SMA, there was a significant reduction in the concentration of oxy-Hb relative to baseline during synchronized tapping when going from the pacing to the continuation phase.

3.4. Contrast maps

In order to illustrate our findings relative to those of Jantzen et al. (2004), we include contrast maps from both data sets (Fig. 5). To obtain fNIRS maps, the raw optical data for all participants first was converted to the oxygenated and deoxygenated concentrations using modified Beer-Lambert law. We then applied a canonical model to estimate the coefficients of the mixed-effect regression model in order to generate a hemodynamic response function for all 55 channels. The channels were configured based on our probe montage using the standard 10 − 10 EEG system. We used a multiple hypothesis testing method with a false discovery rate to adjust the type-I error rate and consequently, generate the ROIs. Finally, all significantly active channels were projected onto a 3-D brain model using AtlasViewer software, which performs image reconstruction and probe registration corresponding to the standard channel positions. Fig. 5A and 5C show the contrast maps from the Jantzen et al. (2004) study, highlighting significant main effects by region based on the MNI coordinates listed in Table 1. These researchers observed a main effect for tapping phase (pacing vs. continuation) and for tapping pattern (synchronization vs. syncopation). The corresponding fNIRS contrast maps are shown in Fig. 5B and 5D. An estimation of MNI coordinates is available in Table 2 based on our mapping of the EEG standard electrode positions to ROIs using AtlasViewer. The contrast maps illustrate consistency between our results and those of Jantzen et al. (2004), as well as some differences, which likely have to do with differences in the nature of thresholding across the two types of data (BOLD vs. oxy-Hb).

4. Discussion

Our goal in the current study was to use fNIRS to replicate and extend findings on the cortical hemodynamics underlying a motor timing task obtained using fMRI (Jantzen et al., 2004). Consistent with Jantzen et al.'s results, overall tapping performance was better (more accurate) for the synchronization than syncopation conditions, with mean performance in the syncopated continuation condition the poorest of the four. As in the Jantzen et al. (2004) study, our results demonstrate that the cortical areas recruited in the performance of a finger tapping task not only reflect the temporal and motor demands of the task itself, but also are strongly influenced by how the required temporal interval was initially established. During the syncopated

Table 1
Brain regions showing significant BOLD contrast effects highlighted in Fig. 5A and 5C ($p < 0.05$) (*data adapted from* Jantzen et al. (2004)).

fMRI Hemisphere	*x*	*y*	*z*	Vol, cm^3	Brodmann's	ROI
Pacing > Continuation						
L	−47	−21	11	6.99	41	STG
R	52	−20	15	5.05	40	STG
Syncopation > Synchronization						
B	0	3	46	5.67	32	SMA
L	−10.4	65.3	57.4	3.28	6	MFG
L	−12	−55	61	7.74	7	SPL
L	−28	40	23	5.85	10	MFG
R	62	−22	−6	2.19	21	MTG
R	16	−3	20	2.26	–	Caudate
L	−19	−19	7	2.16	–	VPL
L	−14	−37	−17	2.24	–	Culmen
R	28	−43	−28	1.88	–	Culmen
L	−30	−50	−33	2.08	–	Tonsil

Table 2
Brain regions showing significant oxygenated hemoglobin contrast effects highlighted in Fig. 5B and 5D ($p < 0.05$). Estimation of MNI coordinates based on mapping of EEG standard electrode positions to ROI using AtlasViewer.

fNIRS Hemisphere	*x*	*y*	*z*	Channel positions	*t*-value	ROI
Pacing > Continuation						
L	−48	−35	13	FT7–FT9, FT7–T7	4.22	STG
R	39	−33	14	FT8–FT10, FT8–T8	4.36	STG
L	−56	29	47	F1–F3, FC3–F3	5.97	MFG/IFG
L	−4	−16	68	FCz–FC1	−6.54	SMA
B	−3	−67	39	CPz–CP1, CPz–CP2	−6.12	SPL
Syncopation > Synchronization						
L	−46	16	27	F3–FC3	7.34	MFG
R	52	−22	15	FT8–FT10, FT8–T8	3.92	STG
B	−1	2	69	FCz–FC1, FCz–Cz	6.6	SMA
B	0	−5	68	FCz–Cz, CPz–Cz	6.03	S1/M1
L	−42	10	20	FC3–FC	−7.43	IFG
L	−52	−18	12	FT7–FT9, FT7–T7	−6.33	STG
L	−2	6	57	FC1–F1	−7.01	PMC

continuation phase, the pattern of hemodynamic activity was significantly different than that observed during the synchronized continuation phase. When comparing the two continuation phases with their respective pacing equivalents, the common difference was a relative decrease in activity within auditory processing areas, although other significant activation was observed, particularly in the sensory-motor areas. In this regard, the patterns of activation in SMA were significantly different between the synchronization and syncopation conditions during the continuation phase, but not during the pacing phase.

Moreover, there was no significant difference in M1 activation between syncopation and synchronization tapping across the two phases. In the most difficult condition (syncopated continuation), additional significant activation was observed within a small cluster of the right STG that was not seen in the other three conditions. Consistent with the Jantzen et al. (2004) study, these results indicate that the complexity of timing behavior can extend neural activity to a broader region of the cortex, both for motor control and for timing maintenance, in this case based on a previously available external auditory stimulus. Finally, the general pattern of activity observed in the fNIRS-based hemodynamics is consistent with the results obtained from previous studies using fMRI (Jantzen et al., 2004; Lewis et al., 2004; Jäncke et al., 2000; Rao et al., 1997).

Several specific differences between our fNIRS data and the previously reported fMRI data emerged as well. For example, in addition to those areas of activation reported by Jantzen et al. (2004), during synchronized pacing, we observed additional activity in bilateral frontal gyrus (perhaps an attentional effect), along with greater activity in left S1/M1 (for controlling execution of right finger tapping), and PMC (for planned movement). Furthermore, whereas Jantzen et al. (2004) found no significant activation differences between their pacing and continuation syncopation conditions, we observed that syncopated pacing resulted in activity in left MTG and MFG, as well as a reduction in the concentration of oxy-Hb in left SMA and right SPL relative to baseline. Although the reason for these differences will need to be investigated further, differences in our study design parameters (seating position, movement rate, and number of tapping cycles) likely contributed. Another factor is the difference between the two imaging modalities. Both fMRI and fNIRS provide a means for indirectly measuring neuronal activity, as both measure changes in cerebral blood volume, a byproduct of neuronal excitation/inhibition. Distinctions include the fact that fMRI has a far superior spatial resolution, as well as the ability to examine blood volume changes throughout the brain and not just at the level of the cortex. In contrast, fNIRS has a somewhat higher temporal resolution, but its area of interrogation is limited to the cortex. Indeed, differences between our results and those observed by Jantzen et al. (2004) are likely due to those issues as well. Nonetheless, the consistencies across the two sets of results are noteworthy.

Overall, cortical activation was broader during syncopated than synchronized pacing, consistent with previous findings (Jantzen et al., 2004; Mayville et al., 2002). Numerous results show that increasingly complex timing behavior is associated with increased cortical activity (basal ganglia, cerebellum) (Harrington et al., 1998; Ivry and Keele, 1989; Serrien, 2008), as is motor planning and motor preparation (SMA, dorsal lateral premotor cortex (DLPMC)) (Mayville et al., 2002), and working memory and attention (PFC, SPL, MTG) (Sarnthein et al., 1998). All four experimental conditions activated a network compatible with the motor-related timing network (M1, PMC, preSMA, and SMA). However, the additional increases and decreases in oxy-Hb in bilateral SMA, left frontal gyrus, premotor, and left MFG observed during the syncopation task indicate increased participation of memory and attention processes and presumably also reflect increased cognitive control. This interpretation is consistent with behavioral findings showing that production of anti-phase patterns imposes higher attentional and cognitive demands than in-phase patterns (Meyer-Lindenberg et al., 2002; Monno et al., 2002). Specific differences in the distributed neural networks engaged across the four conditions included here can thus be explained by differences in the timing and behavioral parameters of the subtasks (Jäncke et al., 1998; Thickbroom et al., 1998). As Jantzen and colleagues observed (Jantzen et al., 2004), both time (in the form of time interval information) and timing (in the form of a sensory-motor relationship) play an integral role in the continuation paradigm.

There are limitations to our study that will need to be addressed in future research. First, there are more complex rhythmic coordination tasks and other rhythmic modalities beyond those used here. Second, our relatively limited number of optodes (16 sources and 20 detectors) limited the cortical regions we were able to measure. In the future, whole head coverage will enable us to differentiate activation in even more detail. Finally, regular improvements to software that supports efficient and effective placement of optodes prior to experimentation via real-time mapping of optode-scalp coupling quality (i.e., PHOEBE) will improve the quality of data acqusition (Pollonini et al., 2016). Interfacing this with fNIRS optode' localizers (i.e., the fOLD toolbox) (Morais et al., 2018) will guide fNIRS optode placement to maximize anatomical specificity based on particular regions of interest. Ultimately, the tolerance to head and body movement unique to fNIRS will allow more complex production of timing based motor behaviors to be performed while hemodynamic activity is monitored simultaneously. The replication and extension of Jantzen and colleagues' (2004) important findings represent an initial step toward pursuing such data.

5. Conclusion

Our findings provide validation of the adequacy of fNIRS as a tool to reproduce and build on well-established fMRI findings of task-elicited cortical activity. In the current study, we demonstrated the neural basis of motor-based timing behavior by exploiting the syncopation-synchronization forms of coordination dynamics, and the continuation phase of maintenance theory demonstrated in earlier work (Jantzen et al., 2004). The hemodynamic response functions we recorded from A1, M1, and SMA are broadly consistent with those reported by Jantzen et al. Finally, we replicated the sensory-motor activation observed by Jantzen et al. in their syncopation vs. synchronization contrast, with syncopated tapping producing broader overall activation and significant increases in the concentration of oxy-Hb in targeted areas relative to synchronous tapping. Taken together, our results validate and extend Jantzen et al.'s observations about the neural basis of timing behavior and the contextual influence of rhythm-based motor behavior, demonstrating that fNIRS can be used to investigate nuanced effects therein.

CRediT authorship contribution statement

Ali Rahimpour: Conceptualization, Methodology, Data curation, Formal analysis, Visualization, Writing - review & editing. **Luca Pollonini:** Methodology, Software, Formal analysis, Visualization, Writing - review & editing. **Daniel Comstock:** Methodology, Resources, Writing - review & editing. **Ramesh Balasubramaniam:** Conceptualization, Methodology, Resources, Writing - review & editing. **Heather Bortfeld:** Conceptualization, Methodology, Resources, Writing - original draft, Writing - review & editing, Funding acquisition.

Acknowledgments

The work was partially supported by NIDCDR01 DC010075 to HB, and by NSFBCS 1460633, NSF DGE 1633722 to RB.

References

Aasted, C.M., Yücel, M.A., Cooper, R.J., Dubb, J., Tsuzuki, D., Becerra, L., et al., 2015. Anatomical guidance for functional near-infrared spectroscopy: Atlasviewer tutorial. Neurophotonics 2 (2), 20801.

Abdelnour, A.F., Huppert, T., 2009. Real-time imaging of human brain function by near-infrared spectroscopy using an adaptive general linear model. Neuroimage 46 (1), 133–143.

Balasubramaniam, R., Wing, A.M., Daffertshofer, A., 2004. Keeping with the beat: movement trajectories contribute to movement timing. Exp. Brain Res. 159 (1), 129–134.

Borjkhani, H., Setarehdan, S.K., 2020. Performance assessment of high-density diffuse optical topography regarding source-detector array topology. PLoS One 15 (3), e0230206.

Bortfeld, H., Wruck, E., Boas, D.A., 2007. Assessing infants' cortical response to speech using near-infrared spectroscopy. Neuroimage 34 (1), 407–415.

Bortfeld, H., Fava, E., Boas, D.A., 2009. Identifying cortical lateralization of speech processing in infants using near-infrared spectroscopy. Dev. Neuropsychol. 34 (1), 52–65.

Byblow, W.D., Stinear, C.M., 2006. Modulation of short-latency intracortical inhibition in human primary motor cortex during synchronised versus syncopated finger movements. Exp. Brain Res. 168 (1–2), 287–293.

Chen, J.L., Penhune, V.B., Zatorre, R.J., 2008. Moving on time: brain network for auditory-motor synchronization is modulated by rhythm complexity and musical training. J. Cogn. Neurosci. 20 (2), 226–239.

Chen, H.C., Vaid, J., Boas, D.A., Bortfeld, H., 2011. Examining the phonological neighborhood density effect using near infrared spectroscopy. Hum. Brain Mapp. 32 (9), 1363–1370.

Cluff, T., Gharib, T., Balasubramaniam, R., 2010. Attentional influences on the performance of secondary physical tasks during posture control. Exp. Brain Res. 203 (4), 647–658.

Collective, B.M., Shaw, D., 2012. Makey Makey: improvising tangible and nature-based user interfaces. Proceedings of the Sixth International Conference on Tangible, Embedded and Embodied Interaction 367–370.

Comstock, D.C., Balasubramaniam, R., 2018. Neural responses to perturbations in visual and auditory metronomes during sensorimotor synchronization. Neuropsychologia 117, 55–66.

Ebrahimzadeh, E., Shams, M., Rahimpour Jounghani, A., Fayaz, F., Mirbagheri, M., Hakimi, N., et al., 2019. Epilepsy presurgical evaluation of patients with complex source localization by a novel component-based EEG-fMRI approach. Iran. J. Radiol. 16 (Special Issue).

Harrington, D.L., Haaland, K.Y., Knight, R.T., 1998. Cortical networks underlying mechanisms of time perception. J. Neurosci. 18 (3), 1085–1095.

Hoppes, C.W., Sparto, P.J., Whitney, S.L., Furman, J.M., Huppert, T.J., 2018. Functional near-infrared spectroscopy during optic flow with and without fixation. PLoS One 13 (3).

Huppert, T.J., 2016. Commentary on the statistical properties of noise and its implication on general linear models in functional near-infrared spectroscopy. Neurophotonics 3 (1), 10401.

Irani, F., Platek, S.M., Bunce, S., Ruocco, A.C., Chute, D., 2007. Functional near infrared spectroscopy (fNIRS): an emerging neuroimaging technology with important applications for the study of brain disorders. Clin. Neuropsychol. 21 (1), 9–37.

Ivry, R.B., Keele, S.W., 1989. Timing functions of the cerebellum. J. Cogn. Neurosci. 1 (2), 136–152.

Jahani, S., Berivanlou, N.H., Rahimpour, A., Setarehdan, S.K., 2015. Attention level quantification during a modified stroop color word experiment: an fNIRS based study. In: Proceedings of the 22nd Iranian Conference on Biomedical Engineering (ICBME). IEEE. pp. 99–103.

Jäncke, L., Specht, K., Mirzazade, S., Loose, R., Himmelbach, M., Lutz, K., Shah, N.J., 1998. A parametric analysis of therate effect'in the sensorimotor cortex: a functional magnetic resonance imaging analysis in human subjects. Neurosci. Lett. 252 (1), 37–40.

Jäncke, L., Loose, R., Lutz, K., Specht, K., Shah, N.J., 2000. Cortical activations during paced finger-tapping applying visual and auditory pacing stimuli. Cogn. Brain Res. 10 (1–2), 51–66.

Jantzen, K.J., Steinberg, F.L., Kelso, J.A.S., 2004. Brain networks underlying human timing behavior are influenced by prior context. Proc. Natl. Acad. Sci. 101 (17), 6815–6820.

Karim, H.T., Sparto, P.J., Aizenstein, H.J., Furman, J.M., Huppert, T.J., Erickson, K.I., Loughlin, P.J., 2014. Functional MR imaging of a simulated balance task. Brain Res. 1555, 20–27.

Kasess, C.H., Windischberger, C., Cunnington, R., Lanzenberger, R., Pezawas, L., Moser, E., 2008. The suppressive influence of SMA on M1 in motor imagery revealed by fMRI and dynamic causal modeling. Neuroimage 40 (2), 828–837.

Kobayashi, E., Bagshaw, A.P., Grova, C., Dubeau, F., Gotman, J., 2006. Negative BOLD responses to epileptic spikes. Hum. Brain Mapp. 27 (6), 488–497.

Lewis, P.A., Wing, A.M., Pope, P.A., Praamstra, P., Miall, R.C., 2004. Brain activity correlates differentially with increasing temporal complexity of rhythms during initialisation, synchronisation, and continuation phases of paced finger tapping. Neuropsychologia 42 (10), 1301–1312.

Lin, C.C., Barker, J.W., Sparto, P.J., Furman, J.M., Huppert, T.J., 2017. Functional near-infrared spectroscopy (fNIRS) brain imaging of multi-sensory integration during computerized dynamic posturography in middle-aged and older adults. Exp. Brain Res. 235 (4), 1247–1256.

Mayville, J.M., Jantzen, K.J., Fuchs, A., Steinberg, F.L., Kelso, J.A.S., 2002. Cortical and subcortical networks underlying syncopated and synchronized coordination revealed using fMRI. Hum. Brain Mapp. 17 (4), 214–229.

Meyer-Lindenberg, A., Ziemann, U., Hajak, G., Cohen, L., Berman, K.F., 2002. Transitions between dynamical states of differing stability in the human brain. Proc. Natl. Acad. Sci. 99 (17), 10948–10953.

Mirbagheri, M., Hakimi, N., Ebrahimzadeh, E., Pourrezaei, K., Setarehdan, S.K., 2019. Enhancement of optical penetration depth of LED-based NIRS systems by comparing different beam profiles. Biomed. Phys. Eng. Express 5 (6), 65004.

Mirbagheri, M., Hakimi, N., Ebrahimzadeh, E., Setarehdan, S.K., 2020. Simulation and in vivo investigation of light-emitting diode, near infrared Gaussian beam profiles. J. Near Infrared Spectrosc. 28 (1), 37–50.

Monno, A., Temprado, J.-J., Zanone, P.-G., Laurent, M., 2002. The interplay of attention and bimanual coordination dynamics. Acta Psychol. (Amst) 110 (2–3), 187–211.

Morais, G.A.Z., Balardin, J.B., Sato, J.R., 2018. fNIRS optodes' location decider (fOLD): a toolbox for probe arrangement guided by brain regions-of-interest. Sci. Rep. 8 (1), 1–11.

Noah, J.A., Ono, Y., Nomoto, Y., Shimada, S., Tachibana, A., Zhang, X., et al., 2015. fMRI validation of fNIRS measurements during a naturalistic task. JoVE (J. Vis. Exp.) 100, e52116.

Pollonini, L., Olds, C., Abaya, H., Bortfeld, H., Beauchamp, M.S., Oghalai, J.S., 2014. Auditory cortex activation to natural speech and simulated cochlear implant speech measured with functional near-infrared spectroscopy. Hear. Res. 309, 84–93.

Pollonini, L., Bortfeld, H., Oghalai, J.S., 2016. PHOEBE: a method for real time mapping of optodes-scalp coupling in functional near-infrared spectroscopy. Biomed. Opt. Express 7 (12), 5104–5119.

Rahimpour, A., Dadashi, A., Soltanian-Zadeh, H., Setarehdan, S.K., 2017. Classification of fNIRS based brain hemodynamic response to mental arithmetic tasks. In: Proceedings of the 3rd International Conference on Pattern Recognition and Image Analysis (IPRIA). IEEE. pp. 113–117.

Rahimpour, A., Noubari, H.A., Kazemian, M., 2018. A case-study of NIRS application for infant cerebral hemodynamic monitoring: a report of data analysis for feature extraction and infant classification into healthy and unhealthy. Inform. Med. Unlocked 11, 44–50.

Raichle, M.E., 1994. Images of the mind: studies with modern imaging techniques. Annu. Rev. Psychol. 45 (1), 333–356.

Rao, S.M., Harrington, D.L., Haaland, K.Y., Bobholz, J.A., Cox, R.W., Binder, J.R., 1997. Distributed neural systems underlying the timing of movements. J. Neurosci. 17 (14), 5528–5535.

Repp, B.H., 2005. Sensorimotor synchronization: a review of the tapping literature.

Psychon. Bull. Rev. 12 (6), 969–992.
Repp, B.H., Su, Y.-H., 2013. Sensorimotor synchronization: a review of recent research (2006–2012). Psychon. Bull. Rev. 20 (3), 403–452.
Ross, J.M., Balasubramaniam, R., 2014. Physical and neural entrainment to rhythm: human sensorimotor coordination across tasks and effector systems. Front. Hum. Neurosci. 8, 576.
Santosa, H., Aarabi, A., Perlman, S.B., Huppert, T., 2017. Characterization and correction of the false-discovery rates in resting state connectivity using functional near-infrared spectroscopy. J. Biomed. Opt. 22 (5), 55002.
Santosa, H., Zhai, X., Fishburn, F., Huppert, T., 2018. The NIRS brain AnalyzIR toolbox. Algorithms 11 (5), 73.
Sarnthein, J., Petsche, H., Rappelsberger, P., Shaw, G.L., Von Stein, A., 1998. Synchronization between prefrontal and posterior association cortex during human working memory. Proc. Natl. Acad. Sci. 95 (12), 7092–7096.
Sergent, J., 1993. Mapping the musician brain. Hum. Brain Mapp. 1 (1), 20–38.
Serrien, D.J., 2008. The neural dynamics of timed motor tasks: evidence from a synchronization-continuation paradigm. Eur. J. Neurosci. 27 (6), 1553–1560.
Spencer, N.J., Bywater, R.A.R., Holman, M.E., Taylor, G.S., 1998. Inhibitory neurotransmission in the circular muscle layer of mouse colon. J. Auton. Nerv. Syst. 70 (1–2), 10–14.
Studenka, B.E., Zelaznik, H.N., Balasubramaniam, R., 2012. The distinction between tapping and circle drawing with and without tactile feedback: an examination of the sources of timing variance. Q. J. Exp. Psychol. 65 (6), 1086–1100.
Thickbroom, G.W., Phillips, B.A., Morris, I., Byrnes, M.L., Mastaglia, F.L., 1998. Isometric force-related activity in sensorimotor cortex measured with functional MRI. Exp. Brain Res. 121 (1), 59–64.
Wijeakumar, S., Huppert, T.J., Magnotta, V.A., Buss, A.T., Spencer, J.P., 2017. Validating an image-based fNIRS approach with fMRI and a working memory task. NeuroImage 147, 204–218.
Wilson, T.W., Kurz, M.J., Arpin, D.J., 2014. Functional specialization within the supplementary motor area: a fNIRS study of bimanual coordination. Neuroimage 85, 445–450.
Wing, A.M., Kristofferson, A.B., 1973. Response delays and the timing of discrete motor responses. Percept. Psychophys. 14 (1), 5–12.
Witt, S.T., Laird, A.R., Meyerand, M.E., 2008. Functional neuroimaging correlates of finger-tapping task variations: an ALE meta-analysis. Neuroimage 42 (1), 343–356.
Wolpert, D.M., Ghahramani, Z., 2000. Computational principles of movement neuroscience. Nat. Neurosci. 3 (11), 1212–1217.